

Logical and Geometrical Complementarities between Aristotelian Diagrams

Hans Smessaert¹ and Lorenz Demey²

¹ Department of Linguistics, KU Leuven
Hans.Smessaert@arts.kuleuven.be

² Center for Logic and Analytic Philosophy, KU Leuven
Lorenz.Demey@hiw.kuleuven.be

Abstract. This paper concerns the Aristotelian relations of contradiction, contrariety, subcontrariety and subalternation between 14 contingent formulae, which can get a 2D or 3D visual representation by means of Aristotelian diagrams. The overall 3D diagram representing these Aristotelian relations is the rhombic dodecahedron (RDH), a polyhedron consisting of 14 vertices and 12 rhombic faces (Section 2). The ultimate aim is to study the various complementarities between Aristotelian diagrams inside the RDH. The crucial notions are therefore those of subdiagram and of nesting or embedding smaller diagrams into bigger ones. Three types of Aristotelian squares are characterised in terms of which types of contradictory diagonals they contain (Section 3). Secondly, any Aristotelian hexagon contains 3 squares (Section 4), and any Aristotelian octagon contains 4 hexagons (Section 5), so that different types of bigger diagrams can be distinguished in terms of which types of subdiagrams they contain. In a final part, the logical complementarities between 6 and 8 formulae are related to the geometrical complementarities between the 3D embeddings of hexagons and octagons inside the RDH (Section 6).

Keywords: Aristotelian relations, square of oppositions, hexagon of oppositions, logical geometry, 3D visualisation, subdiagrams, complementarity, embedding

1 Introduction

Aims of the paper. In addition to using diagrams for the visual representation of individual formulae or propositions, logicians also use diagrams to visualize certain relations between formulae from some given logical system. For example, the relations of contradiction, contrariety, subcontrariety and subalternation which hold between a set of logical formulae, are standardly visualised by means of Aristotelian diagrams, such as the well-known square of oppositions. The latter has a rich tradition, originating in Aristotle's work on syllogistics, but it is also widely used by contemporary logicians to visualize interesting fragments of systems such as modal logic, (dynamic) epistemic logic and deontic logic. Furthermore, other Aristotelian diagrams beyond the traditional square have been

studied in detail, the most widely known probably being the hexagon described by Jacoby, Sesmat and Blanché [1–3]. In recent years, several three-dimensional Aristotelian diagrams have been proposed, such as the octahedron, cube or tetrahexahedron. One such 3D representation, namely the rhombic dodecahedron [4–6], henceforth referred to as RDH, visualises the Aristotelian relations between 14 contingent formulae and serves as the general frame of reference for the present paper. Our central aim is twofold, namely (i) to develop strategies for systematically charting the internal structure of the RDH and (ii) to study various complementarities between Aristotelian diagrams inside the RDH. In doing so, we provide a more unified account of a whole range of diagrams which have so far mostly been treated independently of one another in the literature.

The embedding of subdiagrams. The description of the internal structure of the RDH, and more in particular of the various types of complementarities, crucially relies on the idea that smaller diagrams occur inside bigger diagrams. These notions of subdiagram or diagram embedding/nesting have been studied for other types of diagrams as well, more in particular Euler diagrams [7], Venn diagrams [8], spider diagrams [9] or algebra diagrams [10]. The analysis proposed in the present paper is very much in line with the visual grammar or visual syntax approach developed by Engelhardt [11, p. 104] in that “various syntactic principles can be identified in graphics of different types, and the nature of visual representation allows for visual nesting and recursion [...] any object may contain a set of (sub-)objects within the space that it occupies. When this principle is repeated recursively, the spatial arrangement of (sub-)objects is, at each level, determined by the specific nature of the containing space at that level”. Furthermore, the central role of the RDH as the overall Aristotelian diagram in this paper resembles that of the so-called ‘top state’ in work on the syntax and semantics of UML statecharts [12, pp. 327–328] which describes “the set of transitively nested substates of a composite state” and assumes that “in every statechart there is an inherent composite state called the top state which covers all the (pseudo) states and is the container of the states”.

The structure of the paper. In Section 2 we first introduce the Aristotelian relations and the partitioning of logical formulae into ‘pairs of contradictories’ (PCDs). We then present the rhombic dodecahedron for the 3D visualisation of Aristotelian relations between 14 formulae. In the central part of the paper, i.e. Sections 3, 4 and 5, different types of (bigger) diagrams are distinguished on the basis of which types of subdiagrams they contain. In Section 3, three types of Aristotelian squares are characterised in terms of which types of PCDs they contain. In a next step, Section 4 defines different types of hexagons depending on which types of squares are embedded in them. Similarly, the distinction between the two sorts of octagons in Section 5 is based on differences in the nested hexagons. Section 6 then moves from the level of 2D visual representations to that of 3D visualisation: the different ways in which the 14 formulae can be partitioned into a hexagon (6 formulae) and an octagon (8 formulae) are related to the geometrical complementarities between the 3D embeddings of hexagons and octagons inside the RDH.

2 Aristotelian relations in the rhombic dodecahedron

Aristotelian relations. The traditional Aristotelian relations are defined as follows:

φ and ψ are <i>contradictory</i>	iff	$S \models \neg(\varphi \wedge \psi)$	and	$S \models \neg(\neg\varphi \wedge \neg\psi)$,
φ and ψ are <i>contrary</i>	iff	$S \models \neg(\varphi \wedge \psi)$	and	$S \not\models \neg(\neg\varphi \wedge \neg\psi)$,
φ and ψ are <i>subcontrary</i>	iff	$S \not\models \neg(\varphi \wedge \psi)$	and	$S \models \neg(\neg\varphi \wedge \neg\psi)$,
φ and ψ are in <i>subalternation</i>	iff	$S \models \varphi \rightarrow \psi$	and	$S \not\models \psi \rightarrow \varphi$.

Informally, two formulae are **CONTRADICTORY** when they *cannot be true together and cannot be false together*. They are **CONTRARY** when they *cannot be true together but may be false together* and **SUBCONTRARY** when they *cannot be false together but may be true together*. Finally, notice that **SUBALTERNATION** is not defined in terms of the formulae being *true together* or being *false together*, but in terms of *truth propagation*: there is a subalternation from φ to ψ when φ entails ψ but not vice versa.

Pairs of Contradictories. The 16 formulae (up to logical equivalence) from Classical Propositional Logic which can be built by means of unary or binary connectives and two propositional variables p and q , can be partitioned into the following 8 **PAIRS OF CONTRADICTIONARIES** (PCDs), namely 4 PCDs of type C and 4 PCDs of type O:¹

PCDs of type C:	a.	$(p \wedge q)$	b.	$\neg(p \rightarrow q)$	c.	$\neg(p \leftarrow q)$	d.	$\neg(p \vee q)$
	a'.	$\neg(p \wedge q)$	b'.	$(p \rightarrow q)$	c'.	$(p \leftarrow q)$	d'.	$(p \vee q)$
PCDs of type O:	e.	p	f.	q	g.	$(p \leftrightarrow q)$	h.	$p \wedge \neg p$
	e'.	$\neg p$	f'.	$\neg q$	g'.	$\neg(p \leftrightarrow q)$	h'.	$p \vee \neg p$

Furthermore, any two formulae taken from the top row (a-d) in the PCDs of type C are contrary to one another, whereas any two formulae taken from the bottom row (a'-d') are subcontrary to one another. Notice that we will henceforth disregard the PCD containing the two non-contingent formulae in (h-h'), and focus on the 7 PCDs containing the 14 contingent formulae in (a-a') to (g-g').

The rhombic dodecahedron. Various isomorphic 3D visualisations have been proposed for the logical relations between the 14 contingent formulae above. Both the tetra-hexahedral representation of Sauriol [13] and the tetra-icosahedral representation of Moretti [14] take as their starting point the cube to which six pyramids are added, one on each face of the cube². Sauriol makes use of ‘obtuse’ pyramids (whose angle between the base and each of the triangular faces is less than 45°), thus obtaining the convex polyhedron in Figure 1a. Moretti, on the other hand, makes use of ‘acute’ pyramids (whose angle between the base and

¹ The rationale behind these abbreviations is explained in the next subsection.

² A radically different 3D representation, although fundamentally still isomorphic to the ones in Figure 1, is the ‘double’ tetrahedron of Dubois and Prade [15].

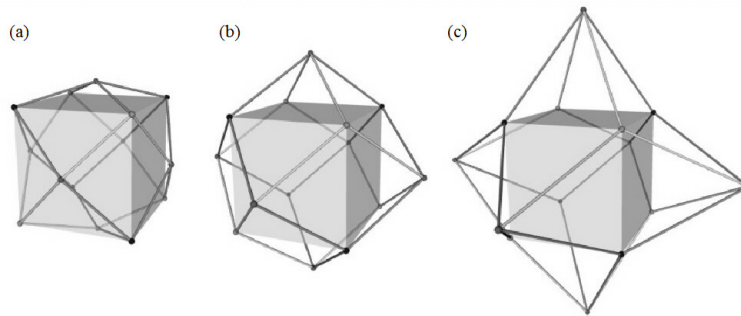


Fig. 1. (a) Sauriol's tetrahexahedron (b) the RDH (c) Moretti's tetraicosahedron

each of the triangular faces is greater than 45°), thus obtaining the concave polyhedron in Figure 1c. The result in both cases is a polyhedron consisting of 24 triangular faces and 14 vertices (corresponding to the 14 formulae), namely the 8 vertices of the cube and the six pyramids' apices. The polyhedron proposed in Smessaert [5, 6] and adopted in Demey [4], by contrast, is the RHOMBIC DODECAHEDRON (RDH) in Figure 1b. It can be considered as lying exactly in between the Sauriol structure in Figure 1a and the Moretti structure in Figure 1c, in the sense that the six pyramids added onto the faces of the cube are 'right' (i.e. having an angle between their base and each of their triangular faces of exactly 45°). As a consequence, each pair of triangular faces of adjacent pyramids falls in the same plane and constitutes a single rhombic face; an RDH thus consists of 14 vertices, but has 12 rhombic faces instead of 24 triangular faces.

Since the RDH is the polyhedral dual of the cuboctahedron (an Archimedean solid combining the properties of a cube and an octahedron [16]), it inherits this double connection, both with the cube and the octahedron. In particular the latter connection is absent from the Sauriol and Moretti structures, and can be seen as the major advantage of the RDH.

The crucial property of the visualisation in Figure 2 is that the Aristotelian relation of contradiction corresponds to central symmetry. In other words, each PCD corresponds to a diagonal through the center of the RDH. Two sets of diagonals can be distinguished: first of all, each formula from the contrariety set in (a-d), with a black label in Figure 2, constitutes a PCD diagonal with a formula from the subcontrary set in (a'-d'), with a grey label. In other words, the 8 vertices with the black and grey labels constitute the cube inside the RDH, and its diagonals represent the 4 PCDs of type C. Secondly, each of the three formulae in (e-g) constitutes a PCD diagonal with its negative counterpart in (e'-g'). Hence, the 6 vertices with a white label constitute the octahedron inside the RDH, the diagonals of which represent the 3 (contingent) PCDs of type O.

Notice that a similar rhombic dodecahedron is used in the visualisation of Zellweger [17]. In comparison to the Aristotelian RDH in Figure 2, however, Zellweger puts the two contingent formulae in (g-g') in the center of his RDH

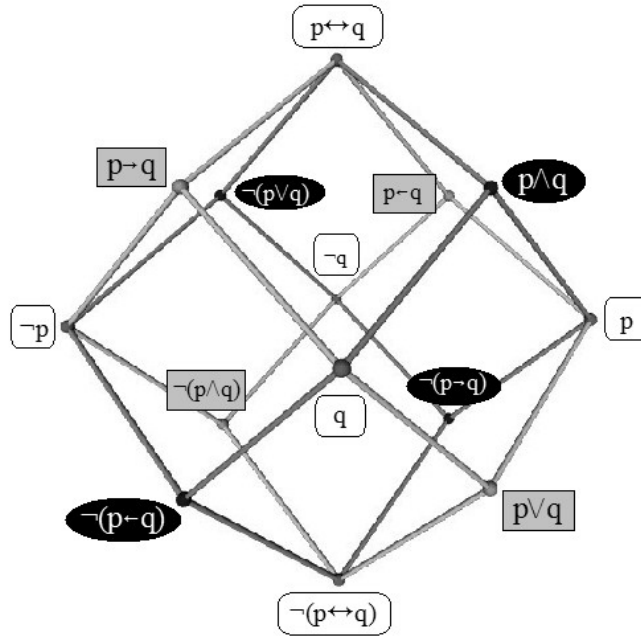


Fig. 2. The 3D visualisation of propositional connectives in the RDH

and the two non-contingent formulae in (h-h') at its top and bottom vertices³. Furthermore, in the Zellweger RDH, all 4 contrary formulae with the black label fall in one plane, all 4 subcontrary formulae with the grey label fall in one plane, and so do all 6 of the white label formulae. We argue elsewhere [18] that, although the Zellweger representation reflects the layered structure of the underlying Hasse diagram more directly, it is less suited for representing the Aristotelian relations.

3 Aristotelian Squares of Opposition

Three types of Aristotelian squares are distinguished in Figure 3. First of all, there are the *classical* squares in Figure 3a-b which have the diagonals for contradiction, the arrows going down for subalternation, the dashed line at the top connecting the contraries and the dotted line at the bottom connecting the subcontraries. There is a crucial difference between these squares in terms of which types of PCDs are involved. The *balanced classical* square in Figure 3a consists of two PCDs that are of the same type, i.e. of type C. The *unbalanced classical* square in Figure 3b, by contrast, consists of one PCD of type C (the diagonal

³ Although the non-contingent formulae in (h-h') are not explicitly represented in our RDH, they can be taken to coincide in its center.

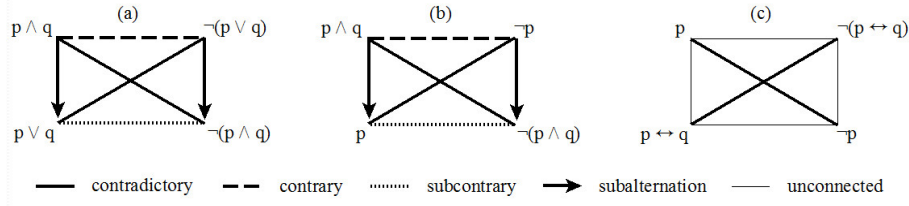


Fig. 3. Aristotelian Squares of Oppositions: (a) balanced classical (b) unbalanced classical (c) degenerate

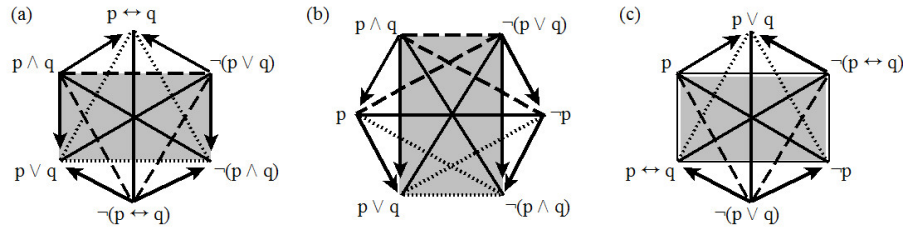


Fig. 4. Aristotelian Hexagons of Oppositions: (a) Jacoby-Sesmat-Blanché = JSB (b) Sherwood-Czezowski = SC (c) Unconnected-4 = U4

from top left to bottom right) and one PCD of type O (the diagonal from bottom left to top right). The third square, in Figure 3c, is *degenerate* in terms of the Aristotelian relations holding between the 4 formulae. Only the diagonals for contradiction remain, whereas the 4 outer edges of the square do not represent any Aristotelian relation whatsoever: the 4 formulae are pairwise ‘unconnected’, i.e. logically independent [19]. Furthermore, the resulting configuration turns out to be balanced again: it consists of two PCDs of the O type⁴.

4 Aristotelian Hexagons of Opposition

In this section, we first distinguish three types of Aristotelian hexagons in terms of which types of PCDs they consist of, namely the Jacoby-Sesmat-Blanché hexagon (JSB hexagon for short), the Sherwood-Czezowski hexagon (SC hexagon) and the Unconnected-4 hexagon (U4 hexagon). Secondly, each of these 3 types of hexagons is further characterized in terms of which types of squares it contains.

Three types of Aristotelian hexagons. The first two hexagons in Figure 4a-b illustrate the two by now standard ways in which a classical Aristotelian square can be extended or generalized to a hexagon [6]. The starting point in both cases

⁴ Another balanced degenerate square can be constructed using the four single-variable formulas p , $\neg p$, q and $\neg q$ (this square is embedded inside the Buridan octagon shown in Figure 8b). Next to these *balanced degenerate* squares, there also exist *unbalanced degenerate* squares. However, the latter play no role in the present paper.

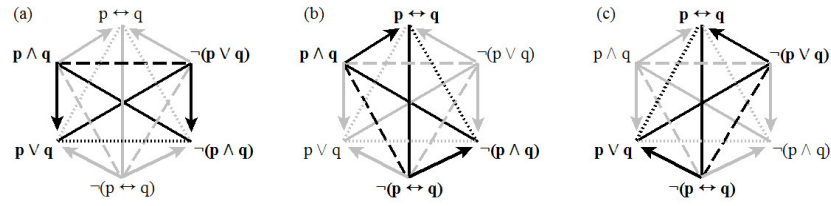


Fig. 5. The Aristotelian squares in the Jacoby-Sesmat-Blanché hexagon JSB

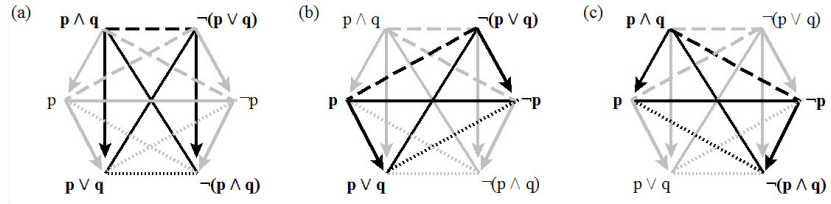


Fig. 6. The Aristotelian squares in the Sherwood-Czezowski hexagon SC

is the balanced classical square of Figure 3a in the grey shaded area, consisting of two PCD diagonals of type C. Furthermore, in both cases the third PCD which is added is of type O. In the JSB hexagon of Jacoby [1], Sesmat [2] and Blanché [3] in Figure 4a the additional PCD consists of the disjunction of the square's upper two vertices and the conjunction of its lower two vertices, and is therefore added to the square 'vertically'. By contrast, in the SC hexagon of Sherwood [20, 21] and Czezowski [22] in Figure 4b, the additional PCD consists of two formulae that are intermediate with respect to subalternation between the square's left two and right two vertices, and is therefore added to the square 'horizontally'. These different ways of inserting the third diagonal into the square result in two fundamentally distinct hexagonal constellations of Aristotelian relations. In the JSB hexagon in Figure 4a, the relations of contrariety and subcontrariety yield two triangles interlocking into a star-like shape inside the hexagon, whereas the arrows of subalternation constitute the outer edges of the hexagon and point from each vertex on the triangle of contraries to the two adjacent ones on the triangle of subcontraries. In the SC hexagon in Figure 4b, by contrast, the arrows of subalternation, which are all pointing downwards, constitute two triangles (of transitivity), whereas the contraries and subcontraries yield two \times shapes instead of two triangles. With the third hexagon in Figure 4c, the starting point is also a balanced square in grey, but this time it is the degenerate square of Figure 3c, consisting of two PCD diagonals of type O. Adding a PCD of type C as the third diagonal in vertical position yields yet another Aristotelian configuration. Because of the presence of the 4 unconnectedness relations in the central square, this hexagon will be referred to as the Unconnected-4 or U4 hexagon⁵. In contrast

⁵ At least two more types of hexagons can be defined: (i) the so-called 'weak' JSB hexagon in Moretti [14] and Pellissier [23] consists of 3 PCDs of type C but is

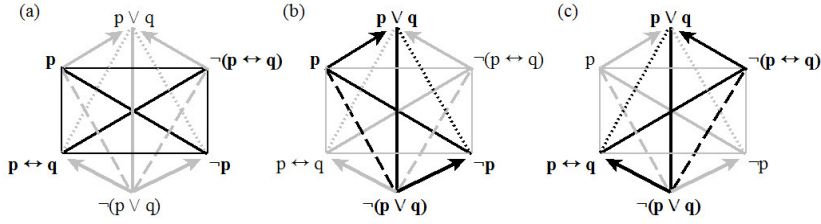


Fig. 7. The Aristotelian squares in the Unconnected-4 hexagon U4

to the JSB and SC hexagons in Figures 4a-b, U4 only contains 4 subalternation arrows instead of 6, and has V-shaped (instead of triangular) constellations for its contraries and subcontraries.

Squares inside the Aristotelian hexagons. We have just distinguished three types of Aristotelian hexagons in terms of which types of PCD diagonals they consist of. A second, closely related strategy for establishing a typology of hexagons is that of considering (i) which types of subdiagrams are embedded inside the bigger hexagonal diagram and (ii) in which way they are embedded. More in particular: any hexagon can be shown to contain 3 squares: since a hexagon consists of three diagonals, each of them can be left out in turn to yield a distinct square (consisting of 2 out of the 3 original diagonals). Looking at the overall constellations in Figures 5 to 7, we observe that all three types of hexagons contain one balanced square in the (a) diagram and two unbalanced classical squares in the (b-c) diagrams. A first difference, of course, is that with the JSB hexagon in Figure 5a and the SC-hexagon in Figure 6a the balanced square is the classical one, whereas with the U4 hexagon in Figure 7a it is the degenerate one. Secondly, although the JSB hexagon and the SC hexagon resemble one another as to which types of squares are embedded, they crucially differ as to the way in which the two unbalanced classical squares are embedded. In Figure 5b-c the embedding involves a rotation of 120° clockwise or counterclockwise (because of the triangular shape of the (sub)contraries), whereas in Figure 6b-c the embedding involves a rotation of only 30° (because of the \times shape of the (sub)contraries). In Smessaert [6] this difference is argued to be due to the fact that the JSB hexagon is closed under the Boolean operations, whereas the SC hexagon is not. In the former case, the hexagon contains the meet and join of any of its pairs of formulae: each vertex on the triangle of contraries is the conjunction or meet of its two neighbours on the triangle of subcontraries, and vice versa, each vertex on the triangle of subcontraries is the disjunction or join of its two neighbours on the triangle of contraries. In the latter case, however, quite a number of pairs of vertices have a meet or join which does not belong to the hexagon (although their negation is always there due to the PCDs). Notice,

isomorphic to the JSB hexagon in Figure 4a, (ii) the so-called Unconnected-12 or U12 hexagon consists of 3 PCDs of type O and, apart from the three diagonals of contradiction, exclusively contains 12 relations of unconnectedness.

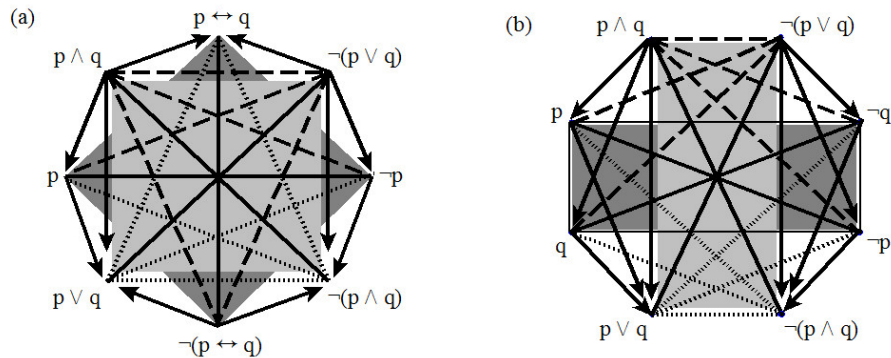


Fig. 8. Aristotelian octagons: (a) Béziau (b) Buridan

by the way, that the U4 hexagon resembles the SC hexagon in not being closed under the Boolean operations either.

5 Aristotelian Octagons of Opposition

In this section two well-known types of Aristotelian octagons will be distinguished, namely the Béziau octagon [24] and the Buridan octagon [25, 26]. They will be shown to differ from one another in terms of the types of hexagons that can be embedded into them as subdiagrams.

The Béziau octagon versus the Buridan octagon. If we adopt the original strategy for distinguishing diagrams, namely on the basis of the types of PCDs they consist of, the two octagons in Figure 8 turn out to be of the same type, since they both contain 2 PCDs of type C as well as 2 PCDs of type O. As a consequence, they can both be seen as combinations of one classical square (with the type C PCDs) in the lighter shade of grey and a degenerate square (with the type O PCDs) in the darker shade of grey. The crucial difference between the two octagons thus concerns the way in which these two squares are embedded into them. With the Béziau octagon in Figure 8a, the vertices of the two squares are strictly alternating on the outer edge, whereas with the Buridan octagon in Figure 8b, they are pairwise alternating. This results in two fundamentally distinct constellations of Aristotelian relations. If we focus on the ‘triangular’ components, the Béziau octagon on the left has two triangles of subalternation as well as an interlocking pair of triangles for contraries and subcontraries. Although the Buridan octagon on the right also contains 4 triangular shapes, they are all of the same type, namely two pairs of subalternation triangles.

Hexagons inside the Aristotelian octagons. So far, the two types of octagons were distinguished in terms of (i) different ways of interlocking the classical and the degenerate squares and (ii) different sets of triangular constellations of Aristotelian relations. The latter strategy for establishing a typology of

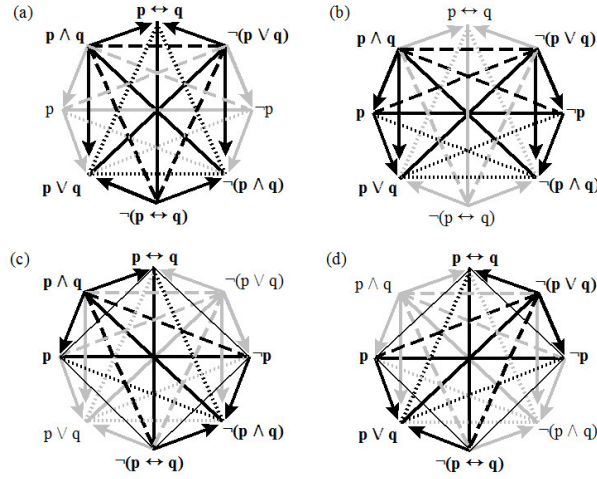


Fig. 9. The Aristotelian hexagons in the Béziau octagon: (a) JSB (b) SC (c-d) U4

octagons naturally leads to that of considering which types of hexagonal sub-diagrams are embedded inside the bigger octagonal diagram. Any octagon can be shown to contain 4 hexagons: since an octagon consists of four diagonals, each of these can be left out in turn to yield a distinct hexagon (consisting of 3 out of the 4 original diagonals). Thus the Béziau octagon can first and foremost be considered as a combination of the JSB hexagon in Figure 9a and the SC hexagon in Figure 9b, with the outer edges completely defined by subalternation arrows. The Buridan octagon, by contrast, is fundamentally a combination of the two SC hexagons in Figure 10a-b, with all the subalternation arrows going downward and two pairs of interlacing \times shapes for the contraries and the sub-contraries. Notice that both with the Béziau octagon and the Buridan octagon the two remaining hexagons that can be embedded are of the U4 type. However, with the former in Figures 9c-d the U4 hexagons show up in their standard shape of Figure 4c, i.e. with the subalternation arrows along the edges and the (sub)contrary V-shapes on the inside, whereas with the latter in Figures 10c-d an alternative shape emerges for the U4 hexagons with more acute angles for the subalternation arrows and the (sub)contrary V-shapes.

6 Complementarities in the Rhombic Dodecahedron

Although in the previous three sections the Aristotelian diagrams have gradually become more complex, their visual representation remained two-dimensional, viz. from square to hexagon to octagon. In this section, however, we return to the complete set of 14 contingent formulae from Classical Propositional Logic (with the 7 PCDs introduced in Section 2) and their 3D visualisation inside the RDH. More in particular, we distinguish two different ways in which the

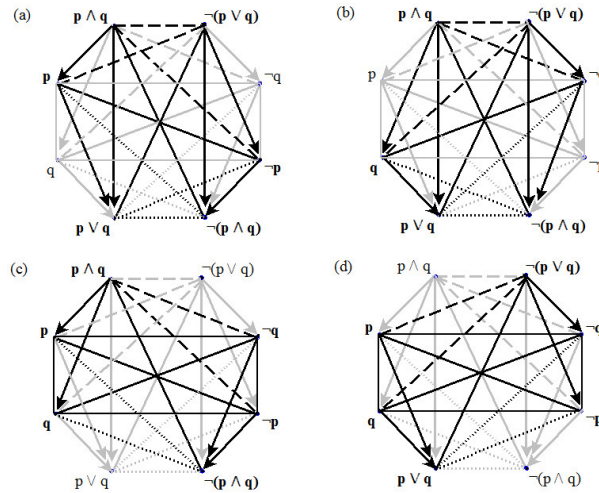


Fig. 10. The Aristotelian hexagons in the Buridan octagon: (a-b) SC (c-d) U4

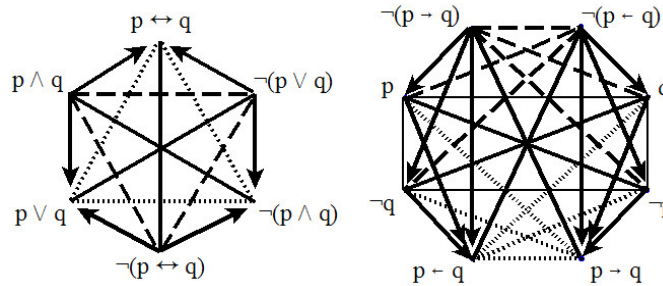


Fig. 11. Logical complementarity between a Jacoby-Sesmat-Blanché hexagon (left) and a Buridan octagon (right)

14 formulae can be partitioned into a hexagon (6 formulae) and an octagon (8 formulae) and relate them to the geometrical complementarities between the 3D embeddings of hexagons and octagons inside the RDH.

Complementarity between the JSB hexagon and the Buridan octagon.

The two diagrams in Figure 11 reveal a first type of logical complementarity: if we take 6 formulae whose Aristotelian relations constitute a JSB hexagon, the 8 remaining formulae yield an Aristotelian octagon of the Buridan type⁶. A number of authors [4–6, 13, 14] have demonstrated that there are exactly six different JSB hexagons embedded inside the RDH. On the left in Figure 12 we

⁶ Since a Buridan octagon is fundamentally a combination of two SC hexagons (see Figure 10a-b), this first logical complementarity can also be seen as holding between a JSB hexagon on the one hand and a pair of SC hexagons on the other.



Fig. 12. 3D geometrical complementarity (middle) between a Jacoby-Sesmat-Blanché hexagon (left) and a rhombicube (right)

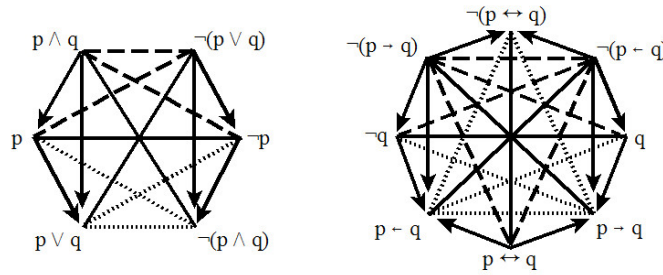


Fig. 13. Logical complementarity between a Sherwood-Czezowski hexagon (left) and a Béziau octagon (right)

see that the embedding of a JSB hexagon constitutes a 2D plane which slices the 3D RDH solid in two equal parts. It can easily be shown that there are indeed exactly six planes that contain 6 out of the 14 vertices (i.e. 3 PCDs) of the RDH. One important result of the present paper is that, for each JSB hexagon in the RDH, the remaining 8 vertices yield a Buridan octagon, whose 3D embedding in the RDH is the solid visualised on the right in Figure 12. This object, which has no standard name in the literature on polyhedra, will be referred to as a **RHOMBICUBE**, the idea being that a cube is put on one of its edges and is squeezed at the top (edge) to the effect that its front and back faces turn from a square into a rhombic shape⁷. The logical complementarity between the JSB hexagon and the Buridan octagon in Figure 11 thus gets a very elegant counterpart in the 3D geometrical complementarity of the hexagon and the rhombicube in the middle of Figure 12.

Complementarity between the SC hexagon and the Béziau octagon. The operation of creating a partition of the 14 formulae can also be performed

⁷ The term does show up occasionally, either as an abbreviation for ‘rhombicuboctahedron’, which is a different, Archimedean solid, or else as a (less felicitous) alternative for the RDH itself.

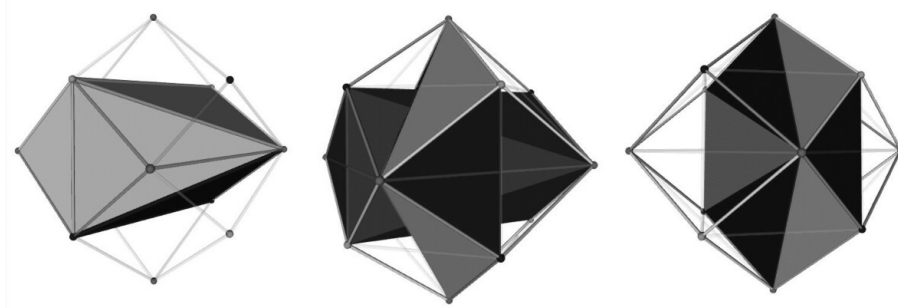


Fig. 14. 3D geometrical complementarity (middle) between a Sherwood-Czezowski hexagon (left) and a Béziau octagon (right)

on the basis of the SC hexagon instead of the JSB hexagon. The two diagrams in Figure 13 thus reveal a second type of logical complementarity: if we take 6 formulae whose Aristotelian relations constitute an SC hexagon, the 8 remaining formulae yield an Aristotelian octagon of the Béziau type. As far as the embedding of an SC hexagon in a 3D polyhedron is concerned, the only proposal, to our knowledge, is that of Sauriol [13, p. 388], who embeds it into his tetrahexahedron. The left diagram in Figure 14 shows the 3D embedding of an SC hexagon in the RDH. This solid is a skew octahedron, i.e. it has 6 vertices and 8 triangular faces. Given that an SC hexagon can be seen as a Buridan octagon with one PCD diagonal left out (see Figure 10a-b), the skew octahedron in Figure 14 can be seen as a rhombicube with 2 vertices (or 1 PCD) ‘sliced off’. Since there are exactly six rhombicubes embedded in the RDH (namely the complements of the six JSB hexagons), and each rhombicube contains two SC octahedra, it follows that there are twelve SC octahedrons inside the RDH. As for its complement, namely the 3D embedding of a Béziau octagon in the RDH, the result on the right in Figure 14 is a squeezed hexagonal bipyramid, which is a solid obtained by sticking together (base to base) two pyramids with a hexagonal base. As a consequence, the logical complementarity between the SC hexagon and the Béziau octagon in Figure 13 has as its counterpart the 3D geometrical complementarity of the octahedron and the hexagonal bipyramid in the middle of Figure 14. Although, from a strictly logical point of view, the complementarities in Figures 11 and 13 are on a par, there is a considerable difference, as far as the visual appeal is concerned, between the 3D geometrical complementarities in Figures 12 and 14. For example, the former has one central symmetry and three reflection symmetries, whereas the latter only has the central symmetry and one reflection symmetry. The main reason for this geometrical difference is that SC hexagons naturally come in pairs (as rhombicubes); the first complementarity respects this pairing, but the second cuts across it.

7 Conclusions and Prospects

The main aim of this paper has been to provide a more unified account of a range of Aristotelian diagrams, which are in general treated independently of one another in the literature. The central part was devoted to a general strategy for systematically charting the internal structure of the rhombic dodecahedron, which represents the Aristotelian relations in a Boolean closed set of 14 contingent formulae. Three families of squares are distinguished depending on the types of PCDs they consist of, 3 families of hexagons in terms of the types of embedded squares, and 2 families of octagons on the basis of the types of nested hexagons. In a final part two types of logical complementarities have been observed, namely (i) between a JSB hexagon and a Buridan octagon, and (ii) between an SC hexagon and a Béziau octagon. The difference in visual appeal of the corresponding 3D geometrical complementarities supports the claim that the former partition is more natural than the latter. The next step in this research project will be to provide an exhaustive typology (by means of combinatorial analysis) of the Aristotelian subdiagrams of the RDH. Central questions will be (i) how many families of octagons, decagons and dodecagons can be distinguished, and (ii) how many members does each family have (e.g. there are 6 strong JSB hexagons, but 12 SC hexagons inside the RDH).

Acknowledgements The second author is financially supported by a PhD fellowship of the Research Foundation–Flanders (FWO).

References

1. Jacoby, P.: A Triangle of Opposites for Types of Propositions in Aristotelian Logic. *The New Scholasticism* 24(1), 32–56 (1950)
2. Sesmat, A.: *Logique II. Les Raisonnements*. Hermann, Paris (1951)
3. Blanché, R.: *Structures Intellectuelles. Essai sur l'organisation systématique des concepts*. Librairie Philosophique J. Vrin, Paris (1969)
4. Demey, L.: Structures of Oppositions in Public Announcement Logic. In: Béziau, J.Y., Jacquette, D. (eds.) *Around and Beyond the Square of Opposition*, pp. 313–339. Springer, Basel (2012)
5. Smessaert, H.: On the 3D visualisation of logical relations. *Logica Universalis* 3(2), 303–332 (2009)
6. Smessaert, H.: Boolean differences between two hexagonal extensions of the logical Square of Oppositions. In Cox, P., Plimmer, B., and Rodgers, P. (eds.) *Diagrammatic Representation and Inference. LNCS 7352*, pp. 193–199. Springer, Berlin/Heidelberg (2012)
7. Fish, A. and Flower, J.: Euler Diagram Decomposition. In: G. Stapleton, G., Howse, J. and Lee, J. (eds.): *Diagrams 2008, LNAI 5223*, pp. 28–44. Springer, Berlin/Heidelberg (2008)
8. Flower, J., Stapleton, G. and Rodgers, P.: On the drawability of 3D Venn and Euler diagrams. *Journal of Visual Languages and Computing* (2013)

9. Urbas, M., Jamnik, M., Stapleton, G., and Flower, J.: Speedith: A Diagrammatic Reasoner for Spider Diagrams. In: Cox, P., Plimmer, B., and Rodgers, P. (eds.) *Diagrammatic Representation and Inference*. LNCS 7352, pp. 163–177. Springer, Berlin/Heidelberg (2012)
10. Cheng, P.C.H.: Algebra Diagrams: A HANDi Introduction. In: Cox, P., Plimmer, B., and Rodgers, P. (eds.) *Diagrammatic Representation and Inference*. LNCS 7352, pp. 178–192. Springer, Berlin/Heidelberg (2012)
11. Engelhardt, Y.: Objects and Spaces: The Visual Language of Graphics. In: Barker-Plummer D. et al. (eds.): *Diagrams 2006*, LNAI 4045, pp. 104–108. Springer, Berlin/Heidelberg (2006)
12. Jin, Y., Esser, R. and Janneck, J.W.: Describing the Syntax and Semantics of UML Statecharts in a Heterogeneous Modelling Environment. In: Hegarty, M., Meyer, B. and Hari Narayanan, N. (eds.): *Diagrams 2002*, LNAI 2317, pp. 320–334. Springer, Berlin/Heidelberg (2002)
13. Sauriol, P.: Remarques sur la théorie de l’hexagone logique de Blanché. *Dialogue* 7, 374–390 (1968)
14. Moretti, A.: The Geometry of Logical Opposition. Ph.D. thesis, University of Neuchâtel (2009)
15. Dubois, D. and Prade, H.: From Blanchés Hexagonal Organization of Concepts to Formal Concept Analysis and Possibility Theory. *Logica Universalis* 6, 149–169 (2012)
16. Coxeter, H.S.M.: *Regular Polytopes*. Dover Publications (1973)
17. Zellweger, S.: Untapped potential in Peirce’s iconic notation for the sixteen binary connectives. In: Hauser N., Roberts D.D. and Evra J.V. (eds.) *Studies in the Logic of Charles Peirce*, pp. 334–386. Indiana University Press (1997)
18. Demey, L. and Smessaert, H.: The relationship between Aristotelian and Hasse diagrams. To appear in the proceedings of *Diagrams 2014*.
19. Smessaert, H. and Demey, L.: Logical Geometries and Information in the Square of Oppositions. Submitted research paper (2014).
20. Khomskii, Y.: William of Sherwood, singular propositions and the hexagon of opposition. In: Béziau, J.Y., Payette, G. (eds.) *New Perspectives on the Square of Opposition*, pp. 43–60. Peter Lang, Bern (2011)
21. Kretzmann, N.: William of Sherwood’s Introduction to Logic. Minnesota Archive Editions, Minneapolis (1966)
22. Czezowski, T.: On certain peculiarities of singular propositions. *Mind* 64(255), 392–395 (1955)
23. Pellissier, R.: Setting n-opposition. *Logica Universalis* 2(2), 235–263 (2008)
24. Béziau, J.Y.: New light on the square of oppositions and its nameless corner. *Logical Investigations* 10, 218–232 (2003)
25. Hughes, G.: The modal logic of John Buridan. In *Atti del Congresso Internazionale di Storia della Logica: La teoria delle modalità*, pp. 93–111. CLUEB, Bologna (1989)
26. Stephen Read, John Buridan’s Theory of Consequence and his Octagons of Opposition. In: Béziau, J.Y., Jacquette, D. (eds.) *Around and Beyond the Square of Opposition*, pp. 93–110. Springer, Basel (2012)